

Interpretation of the magnetic properties of pseudobinary $\text{Sm}_2(\text{Co}, M)_{17}$ compounds. II. Magnetization

R. S. Perkins and S. Strässler

Brown Boveri Research Center, CH-5401 Baden, Switzerland

(Received 13 July 1976)

The data available from paper I of this series offer the opportunity to ascertain the cause of the variations in both Sm^{3+} and transition-metal magnetic moments upon substitution of Co by Fe, Mn, and Cr in $\text{Sm}_2\text{Co}_{17}$. The exchange- and crystal-field parameters derived from the magnetocrystalline anisotropy are used in the calculation of the Sm^{3+} ionic moment in fields of hexagonal symmetry. Both the moment reduction at 0 K and the change in the temperature at which the moment changes sign are found to agree well with the values observed experimentally. The Sm^{3+} ion changes to an $L + S$ type ion at higher temperatures but not at absolute zero. The itinerant-electron moment varies in a manner indicative of electron donation to 3d band in the presence of virtual bound states. The $\text{Sm}_2\text{Co}_{17}$ crystal structure becomes unstable at high 3d-electron concentrations.

INTRODUCTION

Paper I of this series was concerned with the analysis of the magnetocrystalline anisotropy of $\text{Sm}_2(\text{Co}, M)_{17}$ compounds. The subject of this paper is the magnetic moment exhibited by both the transition-metal and samarium atom.

In Paper I a number of references were made to the electronic structure of these alloys. This is dominated by the transition-metal (TM) band structure, upon which the bulk magnetization is sensitively dependent in the eventuality that the Sm moment is small. An analysis of the TM magnetic moment will therefore yield some indications, though not unambiguous ones, of variations occurring in the electronic structure upon cobalt substitution.

The Sm^{3+} ionic moment is also obtained from the measurements of the samarium- and yttrium-based compounds. The value measured represents only a few percent of the bulk magnetization and is therefore subject to rather large experimental uncertainty. However, a variation both between alloys and with temperature is observed which requires explanation. To this end the ionic moment was calculated utilizing the exchange- and crystal-field values derived from the anisotropy investigations of Paper I. The general agreement obtained represents an independent indication of the correctness of these values and an additional confirmation of the sensitivity of the Sm^{3+} moment to its environment.

EXPERIMENTAL AND RESULTS

The materials studied are the same as those of Paper I; namely, $\text{Sm}_2(\text{Co}_{1-x}M_x)_{17}$ and $\text{Y}_2(\text{Co}_{1-x}M_x)_{17}$ with $M = \text{Fe}$ ($0 \leq x \leq 0.4$), Mn ($0 \leq x \leq 0.25$), and Cr ($0 \leq x \leq 0.10$). Details of sample preparation,

characterization, and measurement are also as reported there. The bulk magnetization, M_s , was measured for temperatures between $77 < T < 1000$ K for a number of compositions throughout the series named. The results represent an average of at least four separate samples in each case.

The data for the three Sm series are reproduced in Figs. 1(a)–1(c) which show the temperature and composition dependences $M_s(x, T)$. Figures 2(a)–2(c) contain the molecular moments at 0 K, obtained by extrapolation of the curves in Fig. 1, for both Sm and Y compounds. Figures 3(a)–3(c) indicate the excess in molecular moment per $\text{Sm}_2(\text{Co}, M)_{17}$ molecule over and above that of the corresponding $\text{Y}_2(\text{Co}, M)_{17}$ unit. This has been expressed as the moment per Sm ion. In Figs. 4(a) and 4(b) the temperature and composition dependences of the excess moment per Sm ion are shown normalized at 0 K. The lines have been drawn as a guide only.

THEORY

The Sm^{3+} ion in Sm:Co compounds is subjected to both crystalline electric fields and magnetic exchange fields due to its environment of magnetic and ionized atoms. As has been shown, it is precisely these interactions which are responsible for the rare-earth anisotropy of these compounds. In a similar way their influence upon the Sm atomic-energy levels in the crystal also affects the atomic magnetic moment.

The perturbation theoretical treatment of Paper I is inappropriate for the present case. The reason for this is that mixing into the $J = \frac{5}{2}$ ground state of the $J = \frac{7}{2}, \frac{9}{2}, \dots, \frac{15}{2}$ excited states owing to the crystal and exchange fields substantially alters the calculated ionic moment.¹⁻⁴ Various authors have treated the dependence of the Sm^{3+} moment upon the mentioned interactions.⁴⁻⁶ However, its

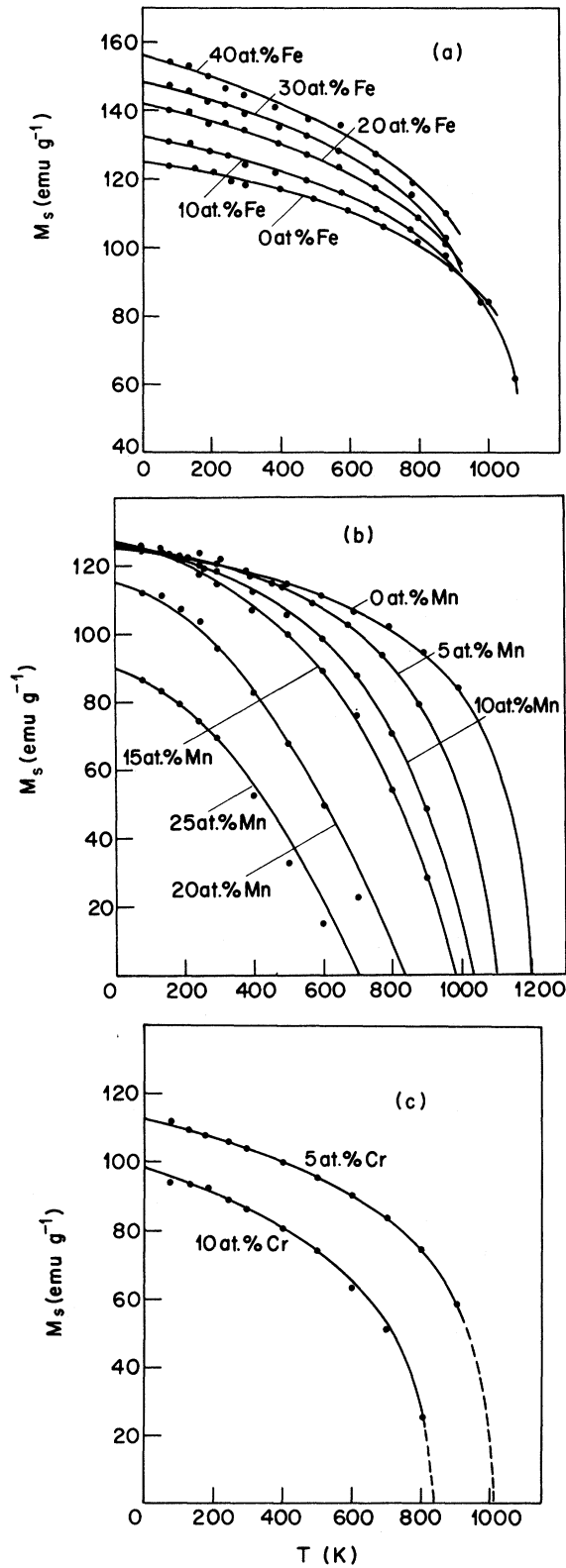


FIG. 1. Saturation magnetization of $\text{Sm}_2(\text{Co}_{1-x}\text{M}_x)_{17}$ compounds. (a) $M = \text{Fe}$; (b) $M = \text{Mn}$; (c) $M = \text{Cr}$.

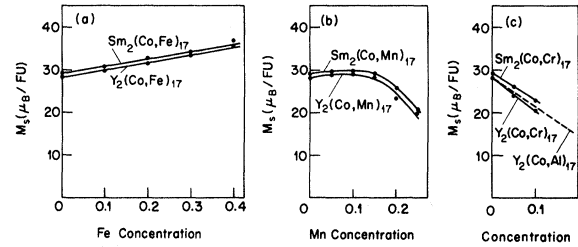


FIG. 2. Magnetic moment per formula unit (FU) at absolute zero for $\text{Sm}_2(\text{Co}_{1-x}\text{M}_x)_{17}$ and $\text{Y}_2(\text{Co}_{1-x}\text{M}_x)_{17}$ alloys where (a) $M = \text{Fe}$; (b) $M = \text{Mn}$, and (c) $M = \text{Cr}$ and Al . Al data originate in Ref. 16.

temperature dependence was not accurately calculated and only a cubic environment was considered. We carry out similar calculations using the Hamiltonian of Paper I [Eq. (1)]:

$$\mathcal{H} = \lambda \vec{L} \cdot \vec{S} + \mathcal{H}_c + 2\mu_B \vec{H}_{\text{ex}} \cdot \vec{S}. \quad (1)$$

The same forms of the spin-orbit, crystal-field, and exchange-field interactions are used as in that case. For the spin-orbit coupling $\lambda = 410$ K was used, corresponding to a $J = \frac{5}{2} - \frac{7}{2}$ energy separation of 1435 K. The assumption is made that the moment lies fully along the z direction which is parallel to the hexagonal c axis. Its value is then

$$\mu = -\mu_B \langle L_z + 2S_z \rangle \quad (2)$$

which may be expressed as

$$\mu = -\mu_B \sum_n \frac{1}{Z} e^{-(E_n/kT)} \langle n | JM \rangle \times \langle JM | J_z + S_z | J'M' \rangle \langle J'M' | n \rangle, \quad (3)$$

where the partition function

$$Z = \sum_n \exp\left(-\frac{E_n}{kT}\right) \quad (4)$$

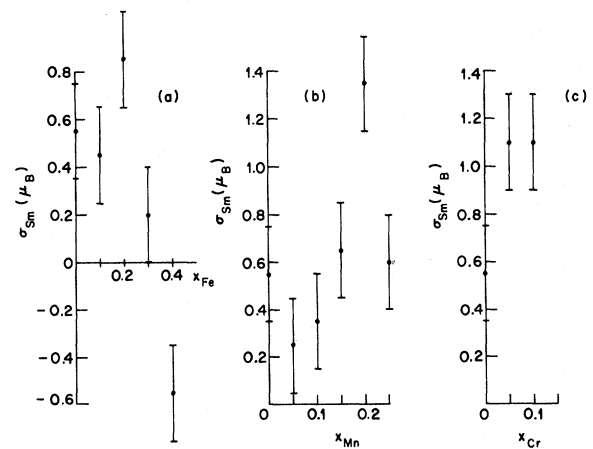


FIG. 3. Excess magnetic moment in $\text{Sm}_2(\text{Co}_{1-x}\text{M}_x)_{17}$ expressed as the Sm^{3+} ionic moment. (a) $M = \text{Fe}$; (b) $M = \text{Mn}$; (c) $M = \text{Cr}$.

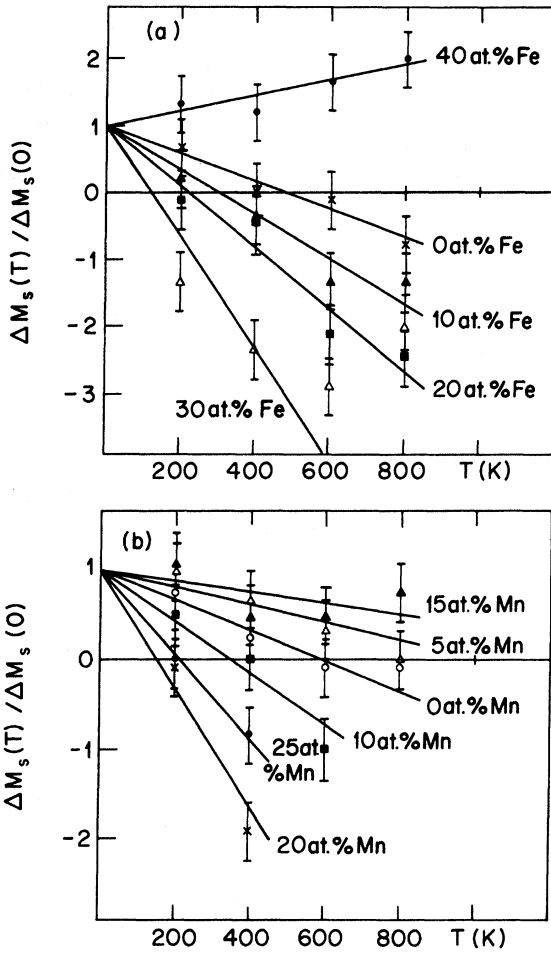


FIG. 4. Normalized temperature dependence of the excess magnetic moment, the Sm^{3+} moment, in $\text{Sm}_2(\text{Co}_{1-x}\text{M}_x)_{17}$ (a) $M = \text{Fe}$; (b) $M = \text{Mn}$.

and E_n , $|n\rangle$ are the energy eigenvalues and eigenfunctions obtained by diagonalizing Eq. (1) between all J, M states from the ground state $J = \frac{5}{2}$ to the highest excited state $J = \frac{15}{2}$. The matrix elements of Eq. (3) are evaluated in the usual manner in terms of $3j$ and $6j$ symbols and reduced matrix elements.⁷ The former were calculated from the appropriate formulas.⁸

J -mixing effects due to crystal and exchange fields and temperature influence the ionic moment to the extent that both its magnitude and sign may be changed.^{5,6} This also applies to the susceptibility, Knight shift, and hyperfine fields.^{2,9}

Figure 5 shows the dependence of the Sm^{3+} ionic moment σ_{Sm} at 0 K upon the crystal field, $\langle r^2 \rangle A_2^0$, and exchange field, $\mu_B H_{\text{ex}}$, parameters appearing in Eq. (1). The temperature dependence of σ_{Sm} shows the expected change in sign⁴ in the 300–400-K range. The precise crossover temperature,

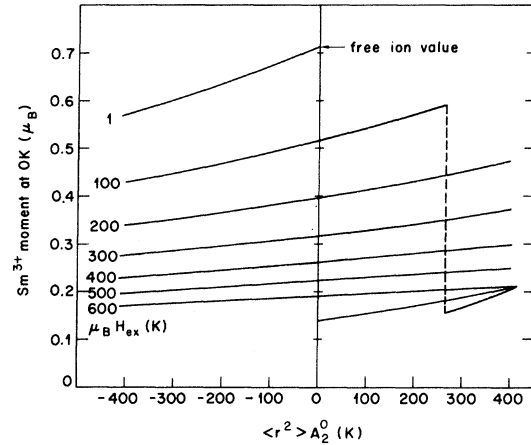


FIG. 5. Calculated dependence of the Sm^{3+} moment at 0 K upon the crystal- and exchange-field parameters $\langle r^2 \rangle A_2^0$ and $\mu_B H_{\text{ex}}$, respectively.

T_{co} , is reproduced in Fig. 6 as a function of $\mu_B H_{\text{ex}}$ and $\langle r^2 \rangle A_2^0$. In this instance the exchange field was kept constant at all temperatures. It may be seen that the Sm^{3+} moment is strongly reduced by both crystal and exchange fields. However, within reasonable limits of $\mu_B H_{\text{ex}}$ and $\langle r^2 \rangle A_2^0$ the moment at 0 K remains positive. This is in marked contrast to the situation for cubic crystal fields^{5,6} in which certain combinations of $\langle r^4 \rangle A_4^0$ and $\langle r^6 \rangle A_6^0$ yield a negative value for the moment at absolute zero. The shifts in the crossover temperature within the same range of values can also be as large as 30%. Whereas the 0 K moment is more sensitive to the exchange field than the crystal field, the reverse is true of the crossover temperature. For negligibly small values of $\mu_B H_{\text{ex}}$ and $\langle r^2 \rangle A_2^0$, the ionic moment is

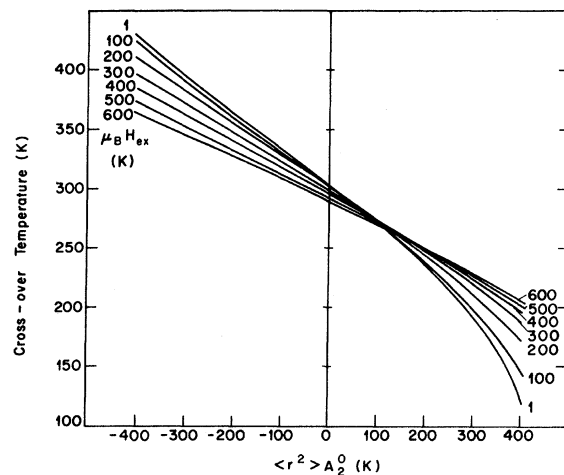


FIG. 6. Calculated dependence of the crossover temperature, T_{co} , upon $\langle r^2 \rangle A_2^0$ and $\mu_B H_{\text{ex}}$.

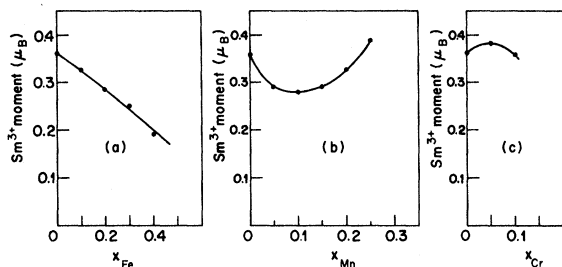


FIG. 7. Composition dependence of the Sm^{3+} moment at 0 K in $\text{Sm}_2(\text{Co}_{1-x}\text{M}_x)_{17}$ compounds calculated with the data of Table II, Paper I. (a) $M = \text{Fe}$; (b) $M = \text{Mn}$; (c) $M = \text{Cr}$.

$0.714\mu_B$, which is the value for the free Sm^{3+} ion.

The sensitivity of both σ_{Sm} and T_{co} to the number of Sm^{3+} excited states used in the calculations should not be overlooked. Changing J_{max} from $\frac{7}{2}$ to $\frac{15}{2}$ decreased σ_{Sm} of $\text{Sm}_2\text{Co}_{17}$ by a further 5% and T_{co} by 14%.

DISCUSSION

The transition-atom moment and Sm^{3+} ionic moment data will be discussed separately.

Samarium moment reduction

The preceding calculations are a satisfactory confirmation of the broad details of the experimental data. The Sm^{3+} moment is indeed dependent upon the prevailing exchange and crystal fields. Furthermore it exhibits a change of sign at higher temperatures which is also composition dependent.

It has been speculated^{5,6} that the lower values of the magnetization of SmCo_5 and $\text{Sm}_2\text{Co}_{17}$ compared to the corresponding yttrium compounds may be explained by crystal-field-induced sign reversal of $\langle L_z + 2S_z \rangle$ to $\langle S_z \rangle$. In fact, for the 2:17 compounds investigated here it appears that this does not happen at 0 K. At room temperature the situation can exist due to the reversal of sign in $\langle L_z + 2S_z \rangle$. The Sm^{3+} ion therefore changes its character as a function of temperature from the $L - S$ type expected of the light rare earths, to $L + S$. Since the Sm spin moment remains coupled antiparallel to the TM moment, the molecular moment is reduced.

The qualitative behavior of the samarium moment in Sm:Co compounds appears then to be correct. However, the presence of the measurements of its magnitude in $\text{Sm}_2(\text{Co}, M)_{17}$ alloys and also of the relevant crystal- and exchange-field parameters allows a quantitative check to be made. For this purpose H_{ex} was assumed to have the same temperature dependence as used in Paper I; namely, that of the TM magnetization taken from the Y-based alloys. The results of the calculation of the ionic moment at absolute zero and of its

normalized temperature dependence for the Fe, Mn and Cr substitution series are reproduced in Figs. 7(a)–7(c) and Figs. 8(a)–8(c), respectively.

Taking into account the large experimental uncertainties present in the data of Figs. 3 and 4, their broad features are in surprisingly good accord with those calculated. $\sigma_{\text{Sm}}(x, 0)$ shows a steady decrease with increasing Fe concentration, but contains a minimum between 5 and 10-at.% Mn content. The moment for the Cr compounds increases with x . Additionally the absolute value of σ_{Sm} is in

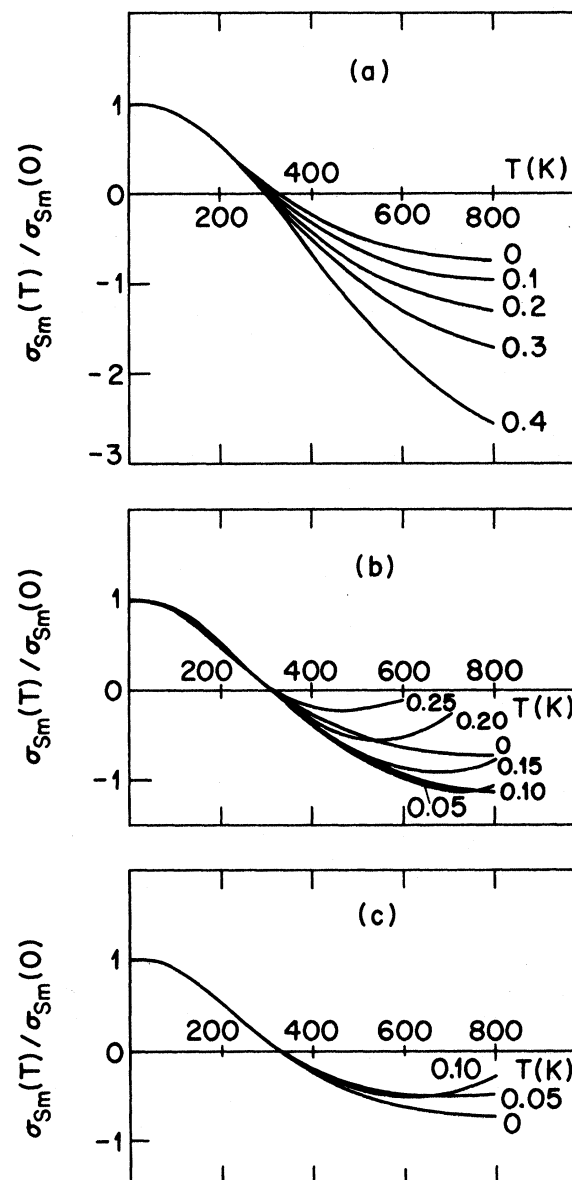


FIG. 8. Calculated normalized temperature dependence of the Sm^{3+} ionic moment in $\text{Sm}_2(\text{Co}_{1-x}\text{M}_x)_{17}$ alloys using the data of Table II, Paper I. (a) $M = \text{Fe}$; (b) $M = \text{Mn}$; (c) $M = \text{Cr}$.

TABLE I. Transition-metal atomic moment in $Y_2(\text{Co}, M)_{17}$ compounds. B is the moment associated with the substituting atom, assuming the Co moment to remain unchanged.

M	$\sigma(\mu_B/\text{transition metal})$	$B(\mu_B/M)$
$Y_2\text{Co}_{17}$	1.65	
10-at.% Fe	1.75	+ 2.7
20-at.% Fe	1.83	+ 2.6
30-at.% Fe	2.00	+ 2.8
40-at.% Fe	2.17	+ 3.0
5-at.% Mn	1.71	+ 2.9
10-at.% Mn	1.72	+ 2.4
15-at.% Mn	1.66	
20-at.% Mn	1.36	
25-at.% Mn	1.16	
5-at.% Cr	1.41	-3.2
10-at.% Cr	1.21	-2.8
16-at.% Al	1.02	-2.3

each case in reasonable agreement. The temperature dependences $\sigma_{\text{Sm}}(x, T)$ are less satisfactory. It seems certain, however, that the discrepancy lies with the experimental data. The crossover temperature decreases with Fe content, but is much less sensitive in the calculated values. At temperatures beyond crossover, the behavior is rather satisfactory for the Fe series, but less so for the Mn data.

Considering the sources of the data used to compare experimental and calculated features of the Sm^{3+} ionic moment, the agreement observed should be considered very satisfactory. As was the case in Paper I, the TM sublattice has been assumed to exhibit identical properties in both the Sm and Y compounds. This may not be the case.

A more obvious source of the discrepancies in the experimental data is conduction-electron polarization associated with the Sm^{3+} and TM ions. In view of the number of factors which influence this phenomenon, it seems inappropriate to consider even the sign of the combined effect.

The experimental Sm^{3+} moment in SmCo_5 also proves to be in satisfactory agreement with the calculated values. Using the data¹⁰ for SmCo_5 and YCo_5 , the zero-degree Sm^{3+} moment is $+(0.29 \pm 0.10)\mu_B$. This compares with the calculated value of $+0.33\mu_B$ with a crossover temperature of 355 K.

Transition-metal moment

The moment per transition-metal atom derived from the $Y_2(\text{Co}, M)_{17}$ data of Fig. 2 is summarized in Table I. For the Fe series the moment behaves in a manner closely related to that of the Co:Fe binary alloys. Its increase corresponds to $1\mu_B$ per $(3d+4s)$ electron decrease. Also the maximum

occurs at a similar composition.¹¹ The majority-spin $3d$ band is therefore full as in pure cobalt, and as indicated by the band structure of SmCo_5 .¹² The cobalt moment reduction from its pure metal value¹³ of $1.72\mu_B$ to $1.65\mu_B$, if significant, results from band-structure, exchange-splitting, or conduction-electron polarization differences.

In contrast the moment behavior in the Cr series does not allow a simple "rigid-band" explanation. If the mean moment is expressed as

$$\bar{\sigma}(x) = \sigma_0 + (B - \sigma_0)x$$

with $\sigma_0 = 1.65\mu_B$ being the Co moment in $Y_2\text{Co}_{17}$ and B is a hypothetical solute moment; then the Cr moment as shown in Table I is approximately $-3\mu_B$. For the Mn series, a value of $+3\mu_B$ is obtained. This behavior closely resembles that of the ternary compounds¹⁴ CoFe:Mn or Cr. The marked difference between Mn and Cr substitution suggests an interpretation involving virtual bound states. One possible explanation is that the Cr $3d$ states are removed to completely above the Fermi level. The Cr valence electrons are therefore donated to both the Co $3d$ band and the conduction band. Mn, however, would retain five majority-spin electrons in a bound state and donate the remaining valence electrons to the $3d$ and conduction bands. The moment reduction beyond 15-at.% Mn corresponds to the minority band becoming full. For $Y_2(\text{Co}, \text{Al})_{17}$,¹⁵ a similar situation is seen to exist in Fig. 2(c) and Table I. Here the Al $3sp$ electrons would be assigned: 2.3 electrons to the $3d$ and 0.7 electrons to the conduction band. A significant difference between the four series is the conduction-electron concentration resulting from solute electron donation.

It should be noted that the 2:17 phase becomes unstable, precisely in the concentration region where the $3d$ band is becoming full. This is a similar observation to that already made in reference to rare-earth transition-metal compounds of 1:5, 2:7, and 1:3 stoichiometry.¹⁶

CONCLUSIONS

The bulk magnetization of $\text{Sm}_2\text{Co}_{17}$ has been investigated under substitution of Co by Fe, Mn, or Cr. The Sm^{3+} moment calculated using the exchange- and crystal-field parameters of Paper I shows a reduction in comparison to the free-ion moment. This is shown to correlate well with the experimental values. The temperature at which the samarium moment becomes negative is also calculated. Whilst the general features agree with the experimental ones, the discrepancies are taken to be indicative of either differences in the transition-metal band structure in the Sm- and Y-based compounds studied, or of the presence of

conduction-electron polarization due to the magnetic rare-earth ion. The overall agreement between the data is an additional confirmation of the validity of the exchange- and crystal-field parameters derived in Paper I from the magneto-crystalline anisotropy.

The influence of crystal fields on the physical properties of samarium compounds has been demonstrated in the case of the ionic magnetic moment and anisotropy. The parameters so obtained may in principle be checked by additional measurements of the low-temperature specific heat, Knight shift or hyperfine field, and paramagnetic susceptibility. Neutron diffraction could also yield the same information in the case of non-Sm or Gd containing alloys. An improved reliability of the data would justify more intensive study of some of the phenomena which have been commented upon in these papers.

The itinerant-electron contribution to the bulk magnetization is found to vary in a manner strongly resembling that of the CoFe:M ternary alloys. The concept of rigid-band filling or emptying combined with virtual bound states appears to be compatible

with the experimental data. The consequence is a strong variation in the conduction-electron concentration. This quantity may also be investigated by such measurements as the plasma frequency and anomalous skin depth. The results would also be of relevance to the determination of both crystal and exchange fields, as has been emphasized in Paper I.

The changes in the band structure in the substitution series are correlated with the phase boundary compositions. The region in which heaviest electron donation to the 3d band occurs is also that in which the 2:17 structure becomes unstable. This is further evidence for the general dependence of rare-earth transition-metal alloy structures upon electron concentration, and of the underlying reason for the similarity in these crystal structures.

ACKNOWLEDGMENTS

The authors have pleasure in acknowledging the support of Dr. A. Menth, and his establishment of the research program in which this work was carried out.

¹S. K. Malik and R. Vijayaraghavan, Phys. Rev. B 10, 283 (1974).

²S. K. Malik and R. Vijayaraghavan, Phys. Rev. B 12, 1098 (1975).

³S. Ofer, E. Segal, I. Nowik, E. R. Baumiger, L. Grodzins, A. J. Freeman, and M. Schieber, Phys. Rev. 137, A627 (1965). Note comment in Ref. 17 of Ref. 1.

⁴J. A. White and J. M. van Vleck, Phys. Rev. Lett. 6, 412 (1961).

⁵K. H. J. Buschow, A. M. van Diepen, and H. W. de Wijn, Phys. Rev. B 8, 5136 (1973).

⁶S. K. Malik and R. Vijayaraghavan, Pramāna 3, 122 (1974).

⁷M. Rotenburg, R. Bivins, N. Metropolis, and J. K. Wotten, Jr., *The 3-j and 6-j Symbols* (MIT Press, Cambridge, Mass., 1959).

⁸A. R. Edmonds, *Angular Momentum in Quantum Mechanics* (Princeton U.P., Princeton, 1961).

⁹H. W. de Wijn, A. M. van Diepen, and K. H. J. Buschow, Phys. Rev. B 7, 524 (1973).

¹⁰H. P. Klein, A. Menth, and R. S. Perkins, Physica B 80, 153 (1975).

¹¹R. S. Perkins and H. Nagel, Physica B 80, 143 (1975).

¹²F. J. Arlinghaus, IEEE Trans. Magn. MAG-10, 726 (1974).

¹³T. Wakiyama, AIP Conf. Proc. 10, 921 (1973).

¹⁴C. W. Chen, Philos. Mag. 7, 1753 (1962); Phys. Rev. 129, 121 (1963).

¹⁵M. Hamano, S. Yajima, and H. Umabayashi, *Proceedings of the Eleventh Rare Earth Conference, Traverse City, Michigan* (United States Atomic Energy Authority Information Commission, Oak Ridge, Tennessee, 1974), p. 477.

¹⁶C. A. Poldy and K. N. R. Taylor, Phys. Status Solidi A 18, 123 (1973); K. N. R. Taylor and C. A. Poldy, J. Phys. F 5, 1593 (1975).